

# Research on the precise recognition stage of cerebral microhemorrhage based on deep learning algorithm

**Pin Lv**

Beijing Jiaotong University, Tianyu Garden in Yuecheng District, Shaoxing City, Zhejiang Province

18457507003@163.com

**Abstract.** Cerebral microbleeds (CMB) is an important type of cerebral microbleeds. In recent years, many studies have proved that CMB can not only cause vascular dementia, but also increase the risk of stroke. Therefore, detection of CMB is of great clinical significance for balancing antithrombotic therapy and risk assessment in stroke patients, and detection of CMB is of great value for diagnosis and prognosis of cranial injury. This paper mainly proposes a two-stage CMB detection framework based on deep learning, which includes the screening stage of brain microhemorrhagic candidate points and the recognition stage of brain microhemorrhagic points based on deep learning. Firstly, in the first stage, we screened CMB candidate points by combining rapid radial transformation and threshold segmentation, and excluded a large number of background regions and obvious non-CMB regions. Then, in the second stage, the two-channel images spliced by sensitivity weighted imaging (SWI) and phase diagram (Pha) were used for false positive judgment by 3D convolutional neural network to distinguish the true CMB from the CMB analog.

**Keywords:** cerebral microbleeds, susceptibility weighted imaging, Convolutional neural network

## 1. Introduction

CMB is a small hemorrhage caused by the rupture of a small blood vessel in the brain or a small blood leakage. After bleeding, hemosiderin is deposited in the space around the small blood vessels in the brain [1]. On MRI-T2-weighted gradient echo or magnetic resonance sensitivity weighted imaging (SWI), uniformly round, mottled low-signal lesions appear [2,3], The automatic detection of CMBS is a very challenging task, first of all, because the distribution of CMBS in the brain is very variable and irregular. Moreover, they are small in size, ranging from 2mm to 10mm in diameter, and there are many CMB analogs in the brain, such as calcifications and veins. Over the past decade, many approaches have been tried to tackle this challenging task. Early studies of CMB automatic detection used morphological features of CMB, such as volume size, geometry, pixel intensity, etc. Therefore, many traditional detection methods based on simple morphological features are not ideal and require a lot of time. Due to the rapid development of deep learning and its unique advantages in the field of image processing, a two-stage convolutional neural network is designed in this paper for CMB detection.

## 2. CMB detection framework principle overview

In order to identify CMB more accurately from the candidate points screened in the first stage, a 3D-CNN network model based on residual network was designed in the second stage. Compared with 2D convolutional neural network, 3D convolutional neural network can better obtain the three-dimensional spatial features of CMB and make the detection results more accurate [4]. The two-stage detection framework is shown in Figure 1.

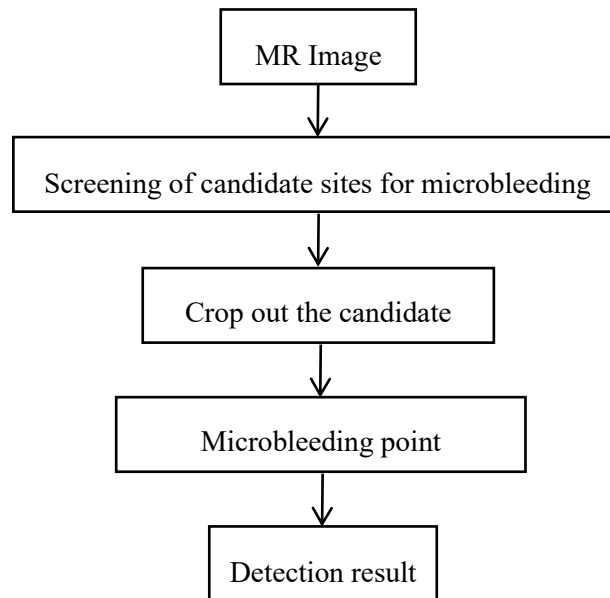


**Figure 1.** Two-stage inspection framework process

## 3. Implementation of CMB detection two-stage detection

### 3.1. Bone removal operation based on ITK

Since the brain microhemorrhagic spots were randomly distributed in the brain and did not appear in the skull, in order to reduce the influence of the skull on the screening results of the brain microhemorrhagic candidate spots before screening, magnetic sensitivity weighted imaging (SWI) was first performed to remove the skull. The boning operation is realized based on ITK, and K-Means clustering algorithm is adopted to achieve automatic segmentation [5]. The results before boning are shown in Figure 2, and the results after boning are shown in Figure 3.

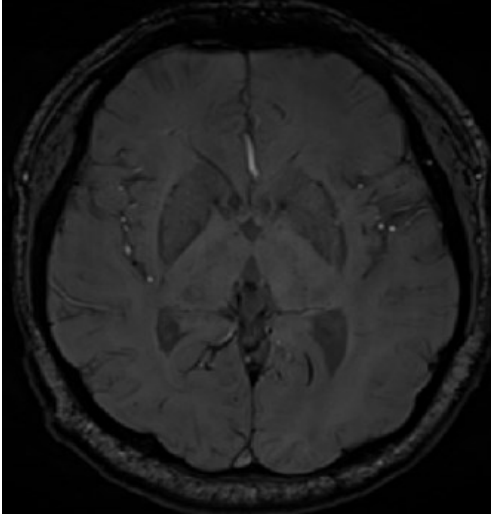


**Figure 2.** SWI image before skull removal

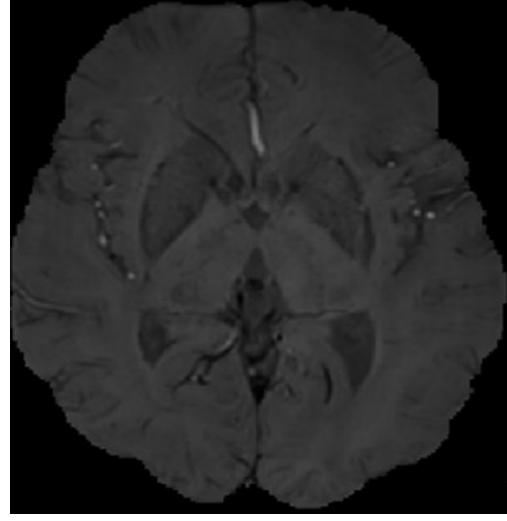


**Figure 3.** SWI image after skull removal

### 3.2. Screening stage of microbleeding candidate points based on traditional algorithm

In this paper, a two-stage algorithm is used to detect CMB. In the first stage, candidate points are screened, and in the second stage, candidate points are classified to find out the real microhemorrhagic points, so that no missing detection can occur in the candidate point screening stage. Considering that CMB is a low-frequency signal on SWI images, and according to the morphological characteristics of CMB, it can be seen that CMB presents circular or oval (non-linear) lesions with a diameter of 2-10mm on SWI images. Therefore, this paper adopts the method of fast radial symmetric transformation algorithm combined with threshold segmentation and morphological features to select candidate points, and adopts the method of combining the two methods to avoid the occurrence of missing detection.

### 3.3. Convolutional neural network implementation

#### 3.3.1. 3D convolutional neural networks

The principle of 3D convolutional neural network is to carry out convolution in three-dimensional space through convolution kernel, and the 3D convolution operation can be expressed by formula 1.

$$V_{xyz} = f \left( \sum_{i=1}^h \sum_{j=1}^w \sum_{k=1}^d w_{ijk} \cdot u_{(x+i)(y+i)(z+k)} + b \right) \quad (1)$$

In the above formula,  $h$ ,  $w$ , and  $d$  are the dimensions of the convolution kernel  $K$ ,  $u$  is the image information,  $b$  is the bias, and  $V_{xyz}$  is the output after convolution.

#### 3.3.2. Parameter number and computational cost of 3D convolutional neural network

When designing a convolutional neural network, it is usually necessary to consider not only the performance of the network, but also the two important factors, the number of parameters and the calculation cost, which will lead to excessive resource consumption.

Therefore, to calculate the parameter number and computation cost of a convolutional neural network, the parameter number and computation cost of a single convolutional layer need to be calculated first.

The formula for calculating the number of single 3D convolution parameters is as follows:

$$Paras = C_{out} \times (K_w \times K_h \times K_d \times C_{in} + 1) \quad (2)$$

Where  $C_{in}$  is the number of channels of input data,  $C_{out}$  is the number of channels of output data, and  $k_h$ ,  $k_w$  and  $k_d$  are respectively the height and width of the convolution kernel. +1 represents the offset term.

Similarly, the computational cost of a single 3D convolution can be calculated using the following formula:

$$FLOPs = 2 \times (K_w \times K_h \times K_d \times C_{in}) \times (C_{out} \times H \times W \times D) \quad (3)$$

Where  $H$ ,  $W$  and  $D$  are the height width and depth of the output data respectively.

### 3.4. Precise identification phase based on deep learning algorithm

The main purpose of this stage is to classify the microhemorrhagic candidates selected in the first stage, so as to distinguish the real microhemorrhagic sites from the similar brain microhemorrhagic analogues. In the first stage, the candidate points with high probability of microbleeding are screened out by the algorithm. Then, in order to reduce the calculation cost, the candidate points selected in the first stage are cut out an image block of  $21 \times 21 \times 21$  with the candidate point position as the center. This size is adopted because the diameter of microbleeding points is 2~10mm, so the size should not be too small, and the microbleeding points must be surrounded. However, it should not be too large, because too large size may produce too much redundant spatial information, affecting the performance of the model.

## 4. Analysis of CMB detection results

### 4.1. Test result evaluation index

CMB detection is a binary classification problem, for which the detection results can be divided into Positive and Negative classes. For the task of CMB detection in this paper, the presence of CMB in the image can be considered as positive (positive class), and the absence of CMB in the image can be considered as false positive (negative class). In the actual test, the following four situations will occur.

Truepositive (TP) : The network predicted CMB, but it was CMB.

There is a Falsepositive (FP) : The network is predicted to be a CMB but is not actually a CMB, a false positive.

Truenegative (TN) : The test is not CMB and is not actually CMB.

Falsenegative (FN) : detects no CMB and is actually CMB, which is a missed detection.

In order to evaluate the performance of the CMB detection method in this paper, Sensitivity (S) and Percision (P) were used to measure the detection effect.

Sensitivity (S), which is Truepositiverate (TPR). It is defined as follows.

$$S = \frac{TP}{TP + FN} \quad (4)$$

The accuracy rate (P), also known as the accuracy rate, represents how many of the predicted positive samples are really positive samples. It is for our predicted results, and its definition is as follows.

$$P = \frac{TP}{TP + FP} \quad (5)$$

The closer the value of the accuracy rate is to 1, the less the number of negative samples are divided into positive samples in the predicted result, that is, the better the classification effect.

The average number of false positives  $FP_{avg}$  is defined as follows:

$$FP_{avg} = \frac{FP}{N} \quad (6)$$

Where,  $N$  represents the total number of subjects in the test set. The average number of false positives represents the number of false positive samples produced on the average recipient, and the smaller the value, the better the classification effect.

#### 4.2. Data set processing

The dataset used in this paper is a dataset for the detection of cerebral microbleeds, including SWI images and Pha images of 480 patients. The dataset was obtained using the Trio Siemens scanner of 3T, which has the following imaging parameters: Repetition time (TR) is 27ms, echo time (TE) is 20ms, turnover Angle (FA) is 15°, pixel bandwidth (BW) is 120HZ/ pixel, volume size is 512×448×72, layer thickness is 2mm, field of view (FOV) is 256×224mm<sup>2</sup>, scanning time is 4.45 minutes. The subjects were drawn from two groups; 214 patients were from stroke patients (mean age standard deviation of 68.2±10.1) and 266 were from older adults with normal aging (mean age standard deviation of 70.1±4.0). Data labeling was performed by a neurologist with 24 years of experience and a neurologist with 12 years of experience.

The data set was divided into a training set, a validation set and a test set. As shown in Table 1, the training set contained data from 340 patients, of which 150 were from stroke patients and 190 were from normal aging elderly people. The validation set contained data from 70 patients, 32 of whom were stroke patients and 38 of whom were aging normally. The test set contained data from 70 patients, including 32 from stroke patients and 38 from older adults who were aging normally.

**Table 1.** Data distribution

Data set	Training set	Validation set	Test set	Totality
Apoplexy	150	32	32	214
Normal aging old people	190	38	38	266
Totality	340	70	70	480

#### 4.3. System implementation

This summary mainly introduces the main hyperparameter Settings in the experiment of software and hardware platforms and deep learning algorithms, including weight initialization method, optimization algorithm and learning rate.

##### 4.3.1. Hardware and software platform

All experiments in this paper were conducted on the same hardware device, in which the operating system was Windows 10 and the GPU was NVIDIA GeForce GTX1080Ti. The FRST algorithm and the algorithm based on the combination of threshold segmentation and geometric methods are implemented by Matlab R2018b. Pytorch framework is used for deep learning training, Python is used in programming languages, and common third-party libraries include OpenCV and Numpy.

##### 4.3.2. Weight initialization

He Keming et al. proposed the He initialization method in 2015. He initialization method effectively solves the problem that Xavier initialization performs poorly on ReLU activation functions, and is also a more commonly used initialization method. Random initialization weights are used in this experiment.

##### 4.3.3. Learning rate

The learning rate size controls the updating speed of network weights. If the learning rate is too small, the network convergence speed is slow, time and computing resources are wasted, and overfitting is easy to occur. If the learning rate is set too large, the loss function may oscillate around the minimum value and fail to converge. Therefore, the learning rate is closely related to the performance of the model. In general, there are two ways to set the learning rate. One is the fixed learning rate, which is set to a fixed value and remains unchanged during the whole training process of the network. The other is variable learning rate, which is constantly changing in the iterative process of the network. Usually, a larger learning rate is selected at the initial stage of training to speed up the convergence speed, and with the continuous iteration, the learning rate slowly declines. In the later stage of training, in order to avoid shock, the learning rate will become smaller and smaller. Learning rate attenuation includes exponential attenuation, fixed value attenuation, step by step attenuation, custom attenuation and so on. The method

of custom attenuation is adopted in this paper. The initial learning rate is 0.001. Decay 90% every 20 epochs.

#### 4.3.4. Optimization algorithm

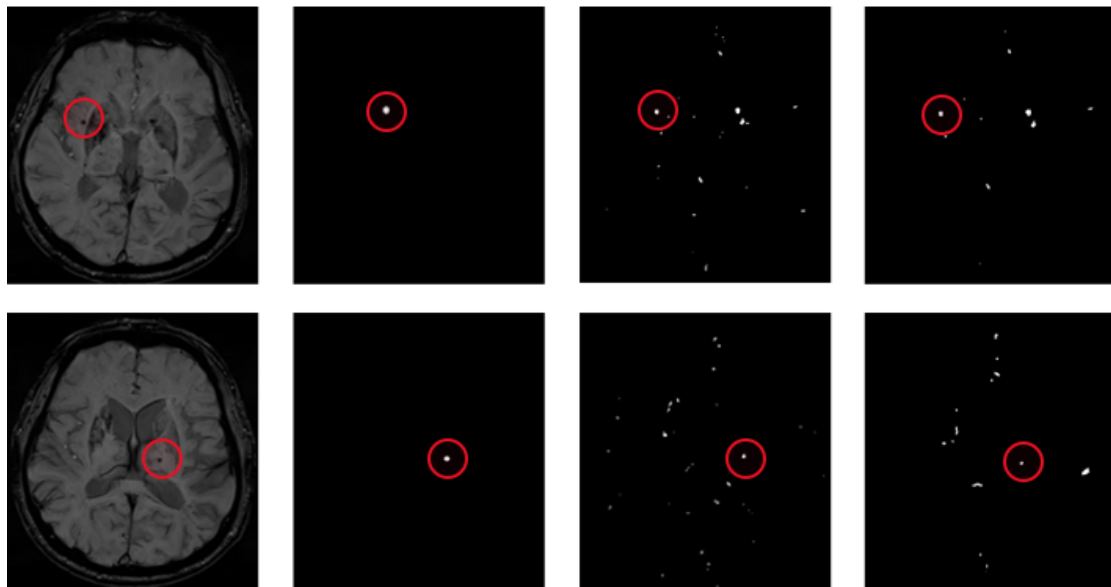
The function of the optimization algorithm is to update the parameters in the network according to the learning rate and loss we get. Gradient descent is an optimization algorithm is an optimization algorithm. It is mathematically understandable that the direction function along the gradient grows the fastest, so the opposite direction of the gradient is the direction in which the function falls the fastest. All optimization algorithms in the field of deep learning need to update parameters according to gradient.

#### 4.4. Experimental results of candidate selection stage

In the candidate point screening stage, this experiment conducted candidate point screening based on the FRST algorithm and micro-bleeding candidate point screening based on the combination of threshold segmentation and geometric methods. It can be seen that the candidate point screening based on the combination of threshold segmentation and geometric methods will produce a large number of false positive samples, which will greatly increase the computational load in the subsequent identification stage. It also wastes a lot of computing time. The results of candidate point screening by FRST algorithm remove a large number of false positive samples, and only retain the CMB candidate region with high probability, which greatly reduces the computational load in the subsequent identification stage.

##### 4.4.1. Screening results of microbleeding candidate points based on threshold segmentation and morphological characteristics

The results of the screening method for microbleeding candidate points based on the combination of threshold segmentation and morphological characteristics are shown in Figure 4. Figure a is the SWI image with CMB in a certain layer of patients, Figure b is the label of CMB marked by doctors, and Figure c is the label of CMB screened by threshold segmentation. The D-diagram is the label of the CMB that is finally screened based on the C-diagram and generated by the constraints such as volume and shape. It can be clearly seen from the figure that through morphological features and constraints such as volume, area and shape, it can be seen that many non-circular and non-circular areas have been removed from the processed image.

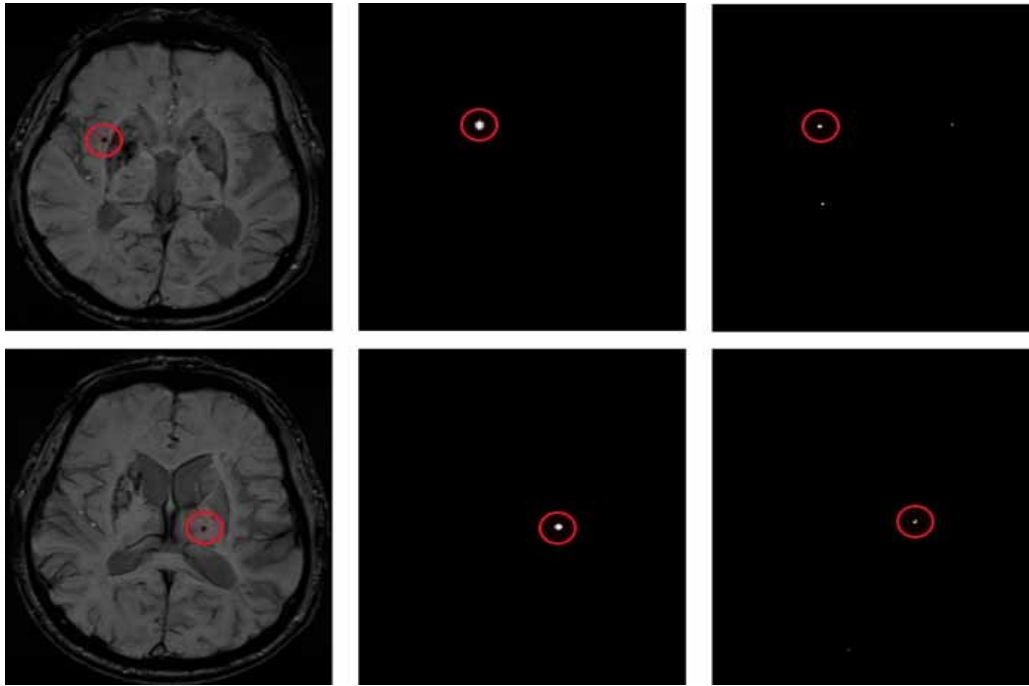


(a) SWI images of patients (b) Doctor's label (c) label for threshold segmentation (d) label after morphological constraint

**Figure 4.** Threshold segmentation and geometric methods filter the results

#### 4.4.2. Screening results of microbleeding candidate sites based on FRST

Screening results of fast radial and symmetric transformation are shown in Figure 5. Figure a is SWI image with CMB in a certain layer of patients, Figure b is label labeled by doctors, and Figure c is label candidate point of CMB selected by using fast radial and symmetric transformation. The fast radial symmetric transformation algorithm can screen out the candidates of brain microhemorrhagic sites, but there are false positive samples in the candidates of CMB.



(a) SWI images of patients (b) Doctor's label (c) label generated by the FRST algorithm  
**Figure 5.** FRST algorithm filtering results

#### 4.4.3. The final candidate selection results

As this paper adopts a two-stage cerebral microhemorrhage detection framework, omissions should be avoided during the screening of candidate points in the first stage, that is, the real microhemorrhagic points are not determined as candidate points, which will lead to the failure of the brain microhemorrhagic spot recognition network in the second stage to obtain the missed microhemorrhagic points, resulting in the omission of the entire framework. Therefore, in this paper, the candidate points selected by threshold segmentation and morphological features are fused with the microhemorrhagic points selected by the fast radial transform algorithm, and then input into the recognition network of the second stage.

#### 4.5. Analysis of the results of microbleeding recognition stage

In the recognition stage, the selected candidate points are mainly classified. In the candidate point screening stage, the selected candidate points include a large number of CMB regions and a small number of non-CMB regions, and the 3D convolutional neural network model is trained to recognize the real CMB region.

### 5. Conclusion

By comparing the experimental results, this paper finds out the most suitable method for screening the candidate points of cerebral microhemorrhagic spot in the first stage. At the same time, the most suitable input size for the second stage is found out through the experiment. Too small input size will lead to incomplete CMB information, and too large input size will lead to excessive redundant information and

reduce accuracy. Finally, the type of input data in the identification stage is determined, and the experiment shows that the combination of SWI and Pha can obtain better detection effect.

## References

- [1] Yan, Wu, Tao, & Chen. (2016). An up-to-date review on cerebral microbleeds. *Journal of stroke and cerebrovascular diseases : the official journal of National Stroke Association*, 25(6), 1301-6.
- [2] Haller, S. , Vernooij, M. W. , Kuijter, J. P. A. , Larsson, E. M. , & Barkhof, F. . (2018). Cerebral microbleeds: imaging and clinical significance. *Radiology*, 287(1), 11-28.
- [3] Haller, S. , Haacke, E. M. , Thurnher, M. M. , & Barkhof, F. . (2021). Susceptibility-weighted imaging: technical essentials and clinical neurologic applications. *Radiology*, 299(1), 203071.
- [4] Wilson D, Ambler G, Lee KI, Lim IS, Shiozawa M, Koga M, et al. (2019). Cerebral microbleeds and stroke risk after ischaemic stroke or transient ischaemic attack: a pooled analysis of individual patient data from cohort studies. *Lancet Neurol*, 18:653-665.
- [5] He, K. , Zhang, X. , Ren, S. , & Sun, J. . (2015). Delving deep into rectifiers: surpassing human-level performance on imagenet classification. *IEEE Computer Society*.